2011 IEEE/RSJ International Conference on
Intelligent Robots and Systems
September 25-30, 2011. San Francisco, CA, USA

Noninvasive Brain-Computer Interface-based Control of Humanoid Navigation

Yongwook Chae, Jaeseung Jeong, *Member, IEEE*, and Sungho Jo, *Member, IEEE*

Abstract— **This study proposes an asynchronous noninvasive Brain Computer Interface (BCI) -based navigation system for a humanoid robot, which can behave similarly to a human. In the experimental procedure, each subject is asked to undertake three different sessions: offline training, an online feedback test, and real-time control of a humanoid robot in an indoor maze. During the offline training session, amplitude features from the EEG are extracted using auto-regressive frequency analysis with a Laplacian filter. The optimal feature components are selected by using the Fisher ratio and the linear discriminant analysis (LDA) distance metric. Two classifiers are hierarchically set to build the asynchronous BCI system. During the online test session, the trained BCI system translates a subject's ongoing EEG into four mental states: rest, left-hand imagery, right-hand imagery, and foot imagery. Event-by-event analysis is applied to evaluate the performance of the BCI system. If the test performance is consistently satisfactory, the subject executes the real-time control experiments. During the navigation experiments, the subject controls the robot in an indoor maze using the BCI system while surveying the environment through visual feedback. The results show that BCI control was comparable to manual control with a performance ratio of 81%. The evaluation of the results validates the feasibility and power of the proposed system.**

I. Introduction

A BCI system using noninvasive scalp-recorded EEG measurements is designed to detect the voluntary changes in ongoing brain activity and to translate different mental states into appropriate commands for severely paralyzed people or "locked-in" patients [1]-[3]. EEG-based BCI systems have been developed as a basic communication channel for simple tasks such as controlling a computer cursor [3]-[6] and spelling some words [7]-[12]. To develop more natural and sophisticated interface methods, especially for robot control, P300-based and band power-based BCI analyses have been investigated. The P300 signal is produced when the brain is visually simulated by a target of interest through certain methods such as sudden flashes. Researchers conducted the first EEG-based humanoid robot control experiment [13]. A Fujitsu HOAP-2 humanoid robot selected a target box from between a green and a red box by detecting P300 signals and then conveyed the box to a pre-defined location. Although the result demonstrated successful BCI-based control of the advanced humanoid, the researchers' approach was limited in several aspects: all of the robot motions were pre-programmed, the control capacity was restricted in the number of targets (two boxes), and the timing of the motion commands was controlled by the system and not by a user. Escolano et al. [14] investigated the first EEG-based human brain-actuated teleoperation system. They showed that a human can navigate and visually explore in a remote location using P300-evoked potentials. Their BCI system enhanced the control capacity by designating various mode choices and improved the usability by applying the teleoperation system via the internet protocol. However their approach relies on timing control by the system and not by a user. Brain-controlled wheelchair navigation has also been a research topic of interest [15]-[16]. The P300 is a responsive signal; therefore, the timing of the control depends on the emergence of a desired stimulus. It is more desirable to extract a user's intention directly from pure thought. Band power-based BCI methods have received much attention [3]-[6], [17]-[21] because they attempt to interpret a user's thoughts directly into specific movements [22]. These methods classify specific motor images in a general sense through the power over the frequency range (e.g., mu (8~12Hz) or beta (18~22Hz)). Notably, asynchronous BCI systems allow consecutive interpretation of EEG data [18]-[21]. Millan et al. [21] proposed a combination of an asynchronous BCI with an agent-based model to enrich the control capacity, and they thereby demonstrated the possibility for continuous control of a brain-actuated mobile robot in a complex maze. This state-dependent agent-based model enhanced the stability and accuracy; however, the control capacity and timing were limited to the perceptual states of a specific environment.

We are interested in an approach to be better suited for complicated real-world applications and to provide a more natural control environment for a user. In the sense of robotic system, a humanoid robot navigation control is a good example of real-world task implementation. Furthermore, the humanoid motions are similar to human motions; therefore, a user feels natural as if he or she is moving his or her own body while controlling the robot. Taking into account previous investigations, the asynchronous (self-paced) BCI system is an appropriate choice for executing rapid and complex movements in a control environment that is natural to the user while also making good use of the advanced controllability of a humanoid robot.

Proper feature selection is crucial for good BCI communication. Classification accuracy depends significantly on the suitable features. Previous works have

Manuscript received October 9, 2001. This work was supported in part by KAIST High Risk High Return Project, Korean government under the KRF grant (No. 2010-0015226) and under Human Resources Development Program for Convergence Robot Specialists.

Y. Chae is with the Department of Computer Science, KAIST, Dajeon, Korea (e-mail: chaeyw82@lkaist.ac.kr).

J. Jeong is with the Department of Bio & Brain Engineering, KAIST, Dajeon, Korea (e-mail: jsjeong@kaist.ac.kr).

S. Jo is with the Department of Computer Science, KAIST, Daejeon, Korea (e-mail: shjo@kaist.ac.kr).

explored feature selection methods experimentally [23]-[27]; however, few have employed them in real-world applications such as the control of an intelligent agent. We have attempted to adopt an optimal feature selection strategy for the humanoid robot navigation control.

This work proposes an asynchronous BCI system based on optimal time-channel-frequency selections from EEG recorded from the scalp, which will realize real-time humanoid robot navigation control.

II. METHOD

A. System and Procedure Description

To ensure a strictly real-time process and to employ teleoperated communication, the whole system consists of three sub-systems, as illustrated in Fig. 1: the BCI system, the feedback system, and the control system. During the three main procedures (offline non-feedback training, online feedback test, and real-time control), the system processes three different types of data, i.e., sensed visual information, measured EEG signals, and motion commands.

During the offline non-feedback training session, the feedback system gives a training cue, which indicates one of four mental states. Of the four mental states, one Non-Control (NC) state is named "rest" and three Motor Imagery (MI) states are named "left hand imagery", "right hand imagery", and "foot imagery". The BCI system acquires the EEG data while a subject sits and comfortably looks at the display. Nothing happens for the first 2 s, then cue text (e.g., "rest") and a filled circle appear on-screen to notify the user of the beginning of a trial. After 4 s, the MI session begins. Every 4 s, a cue arrow pops up to indicate one MI state among three. A subject tries to imagine the intended motor task while the BCI system records his or her EEG. The training protocol is repeated. To prevent forecasting, cues are block-randomized.

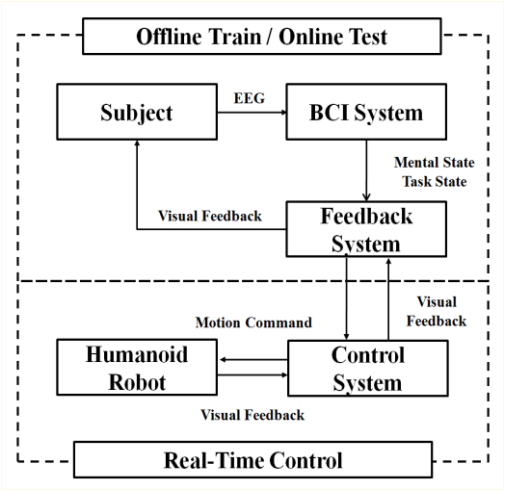

Fig. 1. System architecture. The system consists of three sub-systems: the BCI system, the feedback system, and the control system. During the offline training and online feedback training, the BCI system is tuned through the feedback system. The trained BCI system controls humanoid robot navigation using visual information captured through the robot's vision.

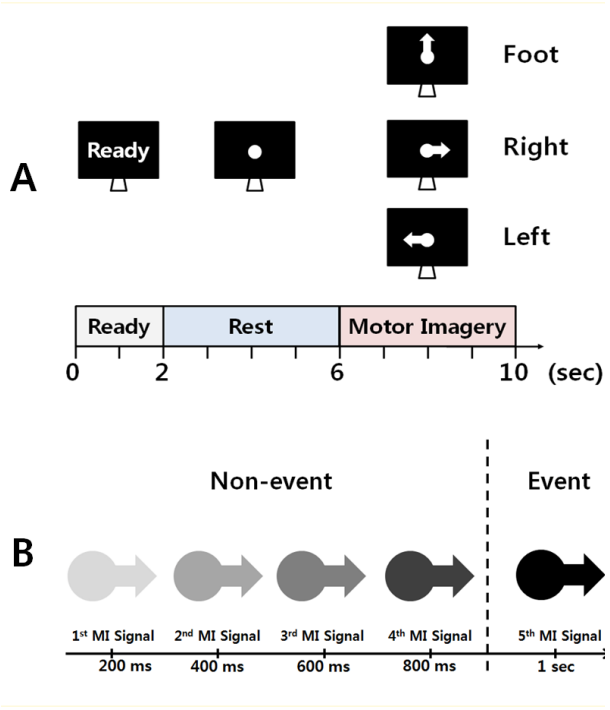

Fig. 2. A) Training protocol: after the ready and rest sessions, the subject is asked to imagine a motor imagery indicated by a cue, which appears on-screen every 4 s. B) Fade-in feedback rule to identify a mental state from EEG: consecutive recognition of a mental state secures a robust selection.

Fig. 2.A illustrates the overall procedure. A subject carries out six offline training sessions over the first two days. Each session consists of two runs and each run is composed of ten trials per task. After the training session, the BCI system analyzes the collected EEG data to extract appropriate features that best classify the mental states and trains two hierarchical classifiers based on the features. The classifiers are used for the real-time control experiment once if the accuracy of the online test is achieved to be above 75%.

During the online feedback test, the trained BCI system extracts a subject's mental state from ongoing EEG signal measurements. The feedback system shows a target cue and a subject tries to imagine the corresponding mental state while his or her EEG signals are recorded. The feedback system identifies a mental state from the EEG signals using a fade-in feedback rule. The fade-in feedback rule is designed to ensure robust control and improve the accuracy of the identification. To avoid abrupt false decisions, a selection level is employed. Whenever classification selects an identical MI state, the selection level increases one degree at a time. Inconsistent state selection or NC state selection decreases the selection level one degree. If the accumulated selection level is above five degree, the MI state selection is confirmed as illustrated in Fig. 2.B. Each session of the feedback test runs 15 trials per task. Once the test performance satisfies the accuracy of above 75%, the subject is ready to execute three real-time control sessions. If the test performance is poor, the subject is again asked to conduct one offline training session to acquire an improved classification.

During the real-time control of a humanoid robot, a subject is asked to control the robot's navigation. The feedback system continuously displays the image sequence acquired from the robot's vision as well as the subject's mental state as interpreted by the feedback system. Meanwhile, the control system regularly transfers a motion command, chosen according to the mental state, to the robot via the TCP/IP wireless system.

B. Data Acquisition and Feature Extraction

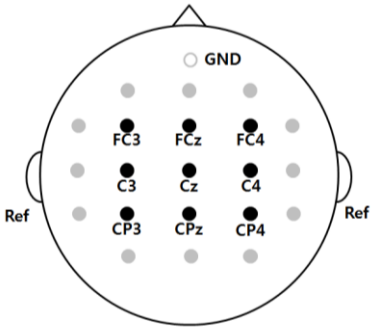

Fig. 3. EEG electrode positions with respect to the international 10-20 system. Electrode positions marked with gray circles are only used in computation of the spatial filter. The nine black circles indicate electrode positions used as main feature channels. All the electrodes are referenced to the left and right mastoids.

During the experiments, the EEG signals of a subject are recorded at a sampling rate of 250 Hz from 21 electrodes (F3, Fz, F4, FT7, FC3, FCz, FC4, FT8, T7, C3, Cz, C4, T8, TP7, CP3, CPz, CP4, TP8, P3, Pz, and P4) as shown in Fig. 3. Sampled EEG signals from 9 channels over the fronto-centro-parietal locations (FC3, FCz, FC4, C3, Cz, C4, P3, Pz and P4) are spatially filtered with the large Laplacian filter [5], [28]. Every 250 ms, the amplitudes in the 4 to 36 Hz band are estimated for 2 s using autoregressive frequency analysis [29] with a model order of 16.

In the offline training session, 32 feature vectors with 288 dimensions (9 channels × 32 frequency components in the band of 4-36 Hz) are collected within the MI and rest periods (4 s for each) for one trial. The feature vectors are used to select informative feature components and train the classifiers. During the online test and real-time control sessions, the feature vectors are sampled every 250 ms and used to classify mental states.

C. Feature Selection

This work proposes an optimal time-channel-frequency selection strategy using the Fisher ratio [23], [25] and linear discriminant analysis (LDA) [30] to designate appropriate features.

1) Fisher Ratio

Given the EEG data from two mental states such as "rest" vs. "left-hand imagery", "rest" vs. "right-hand imagery", or "rest" vs. "foot imagery", a Fisher ratio can be calculated between the two states. Channels and frequencies acquired from the EEG data of a mental state comprise a domain to compute amplitude features through autoregressive frequency analysis. For example with EEG data from the "rest" state and an MI state, let μ_{rest} and σ_{rest} denote the mean and variance, respectively, of the amplitude features computed from the "rest" data, and let μ_{MI} and σ_{MI} denote the mean and variance, respectively, of the amplitude features computed from the MI data. The Fisher ratio is then defined as the ratio of the between-class variance to the within-class variance [23], [25] as follows:

$$fr = \frac{\sigma^2_{between}}{\sigma^2_{within}} = \frac{(\mu_{rest} - \mu_{MI})^2}{\sigma^2_{rest} + \sigma^2_{MI}} \qquad (1)$$

The Fisher ratio is a measure of (linear) discrimination of

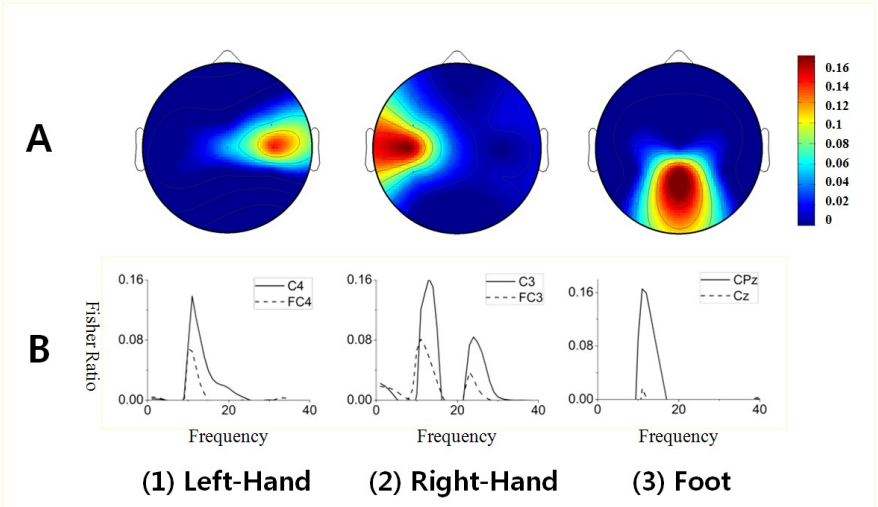

Fig. 4. Optimal channel-frequency selection using the Fisher ratios from the three sets of "rest" vs. MI tasks. (A) Topographical distribution of Fisher ratios of subject A. The first two top-scoring channels for the "left hand imagery" tasks were channels C4 and FC4 while channels C3 and FC3 were selected for the "right hand imagery" tasks and channels CPz and Cz were selected for the "foot imagery" tasks. (B) Spectral distribution of Fisher ratios for subject A. For the "left hand imagery" tasks, the maximum Fisher ratio of C4 was 0.15 at 12 Hz and a 5 Hz window centered at 12 Hz was selected as the optimal frequency region.

two variables and can also be considered as akin to a signal-to-noise ratio. As illustrated in Fig. 4, three different Fisher ratios are estimated from three different amplitude feature sets: "rest" vs. "left-hand imagery", "rest" vs. "right-hand imagery", and "rest" vs. "foot imagery".

2) Optimal Time-Channel-Frequency Selection

This study assumes that a higher Fisher ratio means greater separability. To select the channel-frequency domain that optimally discriminates each MI class, the following method is applied. Among all possible channel-frequency pairs acquired from the EEG data of two mental states ("rest" vs. each of the MIs), a specific channel-frequency pair is found whose Fisher ratio value is the highest. The corresponding channel and a frequency window of 5 Hz centered at the top-scoring frequency are selected to measure the optimal amplitude feature to separate the two mental states. The amplitude value averaged over the window is assigned to be the optimal amplitude feature. For the second top-scoring channel in the Fisher ratio, the same procedure is applied to select the second optimal amplitude feature. According to our system operation scheme, a motor-related time period lasts 4 s (see Fig 2.A). However, the information distribution over the period can be affected by the condition of the subjects and the size of the signal segments used for amplitude estimation. To avoid any noisy periods that were not intended by the subject, optimal time periods are determined for the two mental states by using a LDA classifier. A training data set made up of the two classes is initially divided according to the cued time at 6 s. Signal segments from the training trials between 2 s and 6 s are assigned to the "rest" class and signal segments between 6 s and 10 s are assigned to the "MI" class. The discriminate values of the test sets are averaged over the time, and 1 s intervals centered at a maximum and minimum LDA distance point are selected as the optimal MI period and the optimal rest period, respectively. As the result of feature selection, the feature dimension is reduced to 5 (segments) * 2 (channels) * 1 (averaged frequency). For each channel, an amplitude feature vector is constructed.

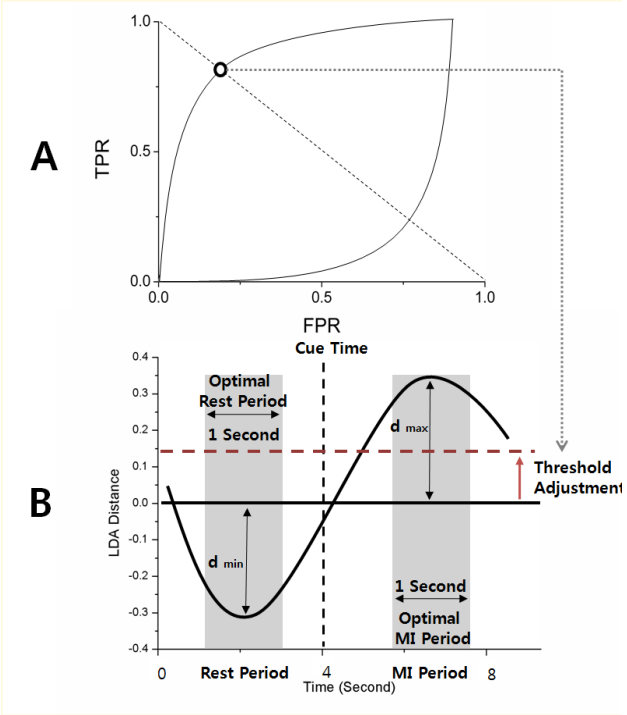

Fig. 5. Optimal time period selection using the LDA distance metric and the determination of a classifier threshold. A) The ROC curve to determine an appropriate threshold value, and B) a typical intention level curve of a subject to discriminate the rest and MI time periods.

D. Classification

To build an asynchronous BCI system that translates the intended directional movements into appropriate movement commands for a humanoid robot, two classifiers called the Intentional Activity Classifier (IAC) and the Movement Direction Classifier (MDC) are hierarchically employed. The IAC classifies between the NC and MI states. If signals are interpreted as the MI state by the IAC, the MDC then classifies which specific MI state is seen from among the "left-hand", "right-hand", and "foot" states.

1) Intentional Activity Classifier (IAC)

As introduced in Section II.C.2), amplitude feature vectors are selected by using the LDA method and the Fisher ratio. The IAC is principally based on the LDA method. As Fig. 5B shows, if the selected features produce a positive LDA distance the corresponding signal is interpreted as an indication of the MI state. Conversely, a negative LDA distance indicates the NC state.

From each trial in the final offline non-feedback training session, two amplitude feature vectors are extracted using the optimal time-channel-frequency selection methods. The MI feature vector is extracted from the MI optimal time period, and the NC feature vector is extracted from the "rest" optimal time period.

Low false-alarm rate is a critical factor to evaluate the control performance of an asynchronous BCI system. To achieve a low rate, we must select and impose an appropriate threshold on the LDA as in Fig. 5.B. To determine a suitable threshold that increases the number of true positive (TP) detections while decreasing the number of false positive (FP) detections, a sample-by-sample receiver operator characteristic (ROC) analysis [19] is used. The two axes of the ROC curve are the true positive rate (TPR) and false negative rate (FPR), respectively, which are both calculated from a threshold. The former is a measure of sensitivity while the later is a measure of selectivity. These quantities are defined as follows:

$$\mathrm{TPR} = \frac{nTP}{nTP + nFN} \qquad (2)$$

$$\mathrm{FPR} = \frac{nFP}{nTN + nFP}$$

where *nTP*, *nFN*, *nTN* and *nFP* are the numbers of true positive, false negative, true negative, and false positive results, respectively. As in Fig. 5A, a TPR value is first found where the TPR is equal to 1-FPR. Then, a point on the ROC that is closest to the TPR value is selected. A threshold that will produce a TPR value at that point is regarded as well-balanced between TPs and FPs [19]. In Fig. 5B, the threshold of the IAC is determined according to this procedure.

2) Motor Direction Classifier (MDC)

When the LDA chooses a true positive result (Section II.D.1), the MDC is applied to the result to indicate the appropriate MI state from among the "left-hand", "right-hand", and "foot" states. The quadratic Fisher's Discriminant Analysis [30] is used to identify the most appropriate MDC. The optimal channel-frequency pair of each class is extracted from the trial data of the final offline non-feedback training session and an optimal time for the MI state is selected using the optimal channel-frequency pair.

Once the IAC and MDC are determined from the training session, they are evaluated in the on-line feedback test, which is discussed in Section III.B.

E. Real-time Control of a Humanoid Robot

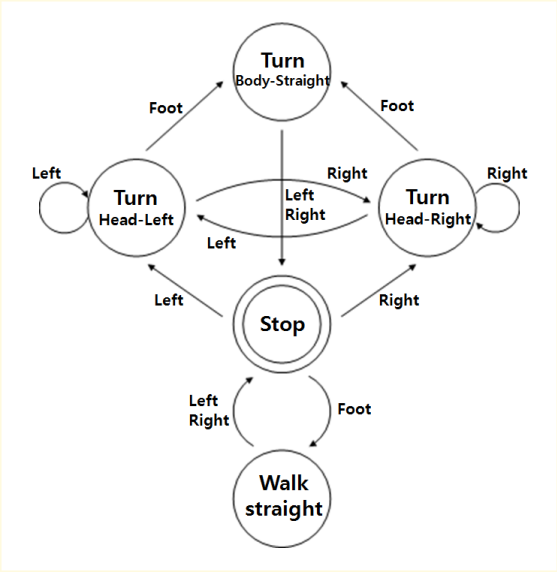

Fig. 6. Diagram of humanoid navigation control. Left: left hand imagery, Right: right hand imagery, and Foot: foot imagery.

A Nao humanoid robot (Aldebran Inc., France) with 25 degrees of freedom is the robot platform used in this work. The monocular vision on its head supplies visual feedback information, which consists of a front view. The control system sends motion commands to the robot and receives visual information from the robot via the wireless TCP/IP protocol every 200 ms. A subject receives two kinds of information from the feedback system on the PC screen: the visual feedback information from the robot and the mental state information interpreted by the BCI system.

The robot walks at a speed of 3.3 cm/s. Its head is allowed to turn left and right to obtain the wide view range. Based on the system constraints, the classifications from the BCI are generated every 250 ms and used to control the robot motion by designed control scheme. Fig. 6 illustrates the navigation control diagram. Five motion commands are programmed to control the robot. If the body and head are facing the same direction, detecting the "foot" state commands the robot to walk forward. If the head and body are facing in different directions, the foot event turns the body to be aligned with the head. A "left hand" or "right hand" state detection stops the robot if it is walking forward, and continued left and right events turn the head to the left or right, respectively, to sense the environment. A left or right turn is achieved by straightening the body after making a left or right turn of the head. It should be noted that our control scheme is different from the state dependent agent-based model [21] because it is designed around postural sensing information and not environmental conditions.

III. RESULTS

Two healthy volunteer male subjects participated in the experiments. Their average age was 26.2 $\pm$ 2.6 years. They had not experienced any prior BCI experiments. The Nao humanoid robot stands on a departure point. It must move to a destination point via waypoint regions. The robot has to move along a designated route in an indoor maze. The route is guided by arrow signs. A subject sees what the robot see through its vision. Using the visual feedback information, the subject controls the robot using the proposed BCI system.

A. Feature Selection

To improve the signal-to-noise ratio and reflect the subject's true mental condition, an optimal time-channel-frequency feature set was selected for each subject as explained in Section II.C. Table I describes the selected feature components of the two subjects "A" and "B". The optimal rest and MI time periods of subject A were between 4.6 s and 5.6 s and between 8.4 s and 9.4 s, respectively. For subject "A", the channel CPz scored highest and the channel Cz scored the second highest in the Fisher-ratios of "rest" vs. "foot-imagery". For subject "B", the two top-scoring channels are reversed. For both subjects, the activations of "left-hand" and "right-hand" imageries are commonly found at C4 and C3, respectively, as previous studies have reported [17], [23]. The optimal frequency set selected from both subject's feature vectors are around mu (8~12Hz) and beta (18~22Hz).

B. Performance of the classifiers

As the classifiers determine the ongoing NC or MI events,

TABLE I
THE RESULT OF FEATURE SELECTION

Subject	Optimal Period (Sec) Rest	Optimal Period (Sec) MI	Task	Channel	Frequency
"A"	4.6-5.6	8.4-9.4	Left	C4	9-13
				FC4	9-13
			Right	C3	11-15
				FC3	9-13
			Foot	CPz	9-13
				Cz	9-13
"B"	4.4-5.4	8.0-9.0	Left	C4	22-26
				FC4	11-15
			Right	C3	9-13
				FC3	9-13
			Foot	Cz	8-12
				CPz	8-12

the classification performance on the online feedback test is evaluated by event-by-event analysis. The number of correctly selected mental events is counted during the test periods. To measure the asynchronous classification, the

numbers of true positive, true negative, false positive, and false negative events are counted to calculate the TPR and the FPR in (2). To measure the MI classification, the average response time (i.e., the mean value of time required to confirm the first event) and the accuracy for each mental task are calculated. Table II summarizes the results. Subjects "A" and "B" were trained using 6 and 5 offline training sessions totaling 180 and 150 trials per class, respectively. Subject "A" achieved a mean TPR of 83.7% and a mean FPR of 4.4%. Subject "B" showed a mean TPR of 90.5% and a mean FPR of 6.9%. The average accuracy of subject "A" was 83.9% while subject "B" achieved 89.3%. The right-hand task for subject "A" and the foot task for subject "B" each resulted in the lowest accuracy among the four tasks. The last column of Table II shows the average response time of each task. The average response time over all of the tasks was 1.74 s for subject "A" and 1.92 s for subject "B".

C. *Control of the Humanoid Robot*

Each subject controlled the robot three times using the proposed BCI system and one time through keyboard touches for comparison. During manual keyboard control, each subject was asked to drive the robot using three keys: up, right, and left. The manual session was performed ahead of the BCI control sessions. The experimental performance is summarized in Table III. The travelled distance, run time, and number of passed waypoints are compared between the manual and mental controls. For the manual control scheme, the run times were 423 s for subject "A" and 412 s for subject "B", and the travelled distances were 513 cm and 542 cm, respectively. For the BCI control scheme, the average run times of three sessions were 529.0 s for subject "A" and 504.6 s for subject "B". The average travelled distances were 530.3 cm for subject "A" and 545.3 cm for subject "B". The ratio of operating times between the two controls was as high as 0.80 for subject "A" and 0.82 for subject "B", and the ratio of operating distances was as high as 0.97 for subject "A" and 0.93 for subject "B". These time and distance ratios demonstrate that the performance of mental control is comparable to that of manual control. Fig. 7 illustrates the robot navigation pathways from departure to the end during the real-time control experiments. The results demonstrate the robot navigated along fairly reasonable pathways without seriously losing direction through the mental control.

TABLE II
THE RESULT OF ON-LINE FEEDBACK TEST

Subject	Trials	TPR (%)	FPR (%)	Task	Acc (%)	Response Time (s)
"A"	180	83.7	4.4	Rest	95.6	1.75
				Left	80.0	1.65
				Right	66.7	1.81
				Foot	93.3	1.76
				Avg.	83.9	1.74
"B"	150	90.5	6.9	Rest	93.0	1.62
				Left	100.0	2.02
				Right	92.9	2.08
				Foot	71.4	1.97
				Avg.	89.3	1.92

TABLE III
THE RESULT OF REAL-TIME NAVIGATION CONTROL OF HUMANOID ROBOT

Subject	Session	Time (s)	Dist. (cm)	Way Point
"A"	Manual	423	513	5/5
	1	502	535	4/5
	2	550	507	5/5
	3	535	549	5/5
	Average	529	530.3	-
"B"	Manual	403	542	5/5
	1	532	551	5/5
	2	483	562	5/5
	3	499	523	5/5
	Average	504.6	545.3	-

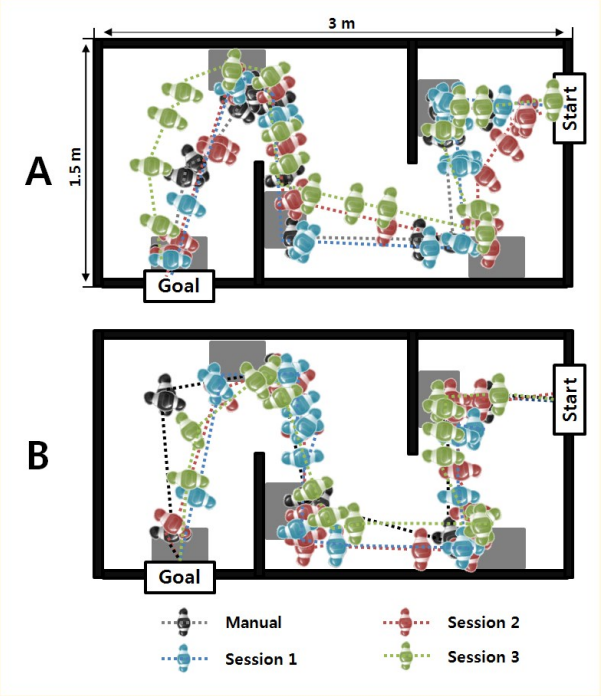

Fig. 7. Humanoid robot navigation pathways. The black dotted line indicates the robot pathway as controlled through the keyboard and the other colored dotted lines illustrate the robot pathways controlled through the BCI system over the 3 sessions. Each robot icon shows the orientation, and each gray box indicates a waypoint region.

IV. DISCUSSION

This paper showed that real-time humanoid robot navigation in an indoor maze was successfully achieved using only mental control by a subject located in a different place.

The proposed system consists of the BCI system, the feedback system, and the control system. Such a division is useful in two main aspects. In teleoperation, a controlled object can operate far from a subject. Hence, localization of the BCI system separately from the control system is efficient. In addition, the division of systems is amenable to the implementation of real-time operation. Processing each sub-system separately makes each one less affected by delays in other sub-systems. The proposed system uses optimal feature selection as well as hierarchical classification to

improve accuracy. Well-organized hierarchical classification based on a good feature set is significantly effective in increasing the number of recognized mental intentions without increasing the number of electrodes or requiring unattractive and complicated algorithms.

The proposed system includes a posture-dependent control architecture, as in Fig. 6, to facilitate the real-time control. We agree with Millan et al. [21] that an automated system is a key feature for efficient BCI control. However, our control model is different from Millan's. Their agent-based robot perceives and executes a command based on the environmental state. Meanwhile, our command control protocol relies on the robot's own postural movements. Hence, our system has the advantage that the decisions are based only on sensing information with no presumptions about the situation. Furthermore, such a posture-dependent control architecture is good to execute various movements.

This study chose a humanoid robot as a test-bed. During navigation, the robot can look around and execute various locomotive motions based on a subject's mere thought. A subject senses visually just what the robot sees, and the robot moves according to the subject's intention. Even though an erroneous movement may be instantly selected, the subject can modify the movement quickly due to the asynchronous control and the visual feedback information.

This work demonstrates the preliminary results of the feasibility of the proposed method. Currently, a few subjects have tested the method. We plan to test the system from more subjects to confirm its performance capability.

REFERENCES

[1] A. Küber, and K. –R. Müller, An introduction to brain computer interfacing, In: Toward brain-computer interfacing, MIT Press, Cambridge, MA, pp. 1-26, 2007.

[2] J. R. Wolpaw, et al. "Brain-computer interface technology: a review of the first international meeting", IEEE Trans. Rehabilitation Engineering, vol. 8, no. 2, pp. 164-173, 2000.

[3] J. R. Wolpaw, N. Birbaumer, D. J. McFarland, G. Pfurtscheller, and T. M. Vaughan, "Brain-computer interfaces for communication and control," *Clin Neurophysiol,* vol. 113, pp. 767-91, Jun 2002.

[4] G. Pfurtscheller, C. Neuper, C. Guger, W. Harkam, H. Ramoser, A. Schlogl, B. Obermaier, and M. Pregenzer, "Current trends in Graz brain-computer interface (BCI) research," *IEEE Transactions on Rehabilitation Engineering,* vol. 8, pp. 216-219, 2000.

[5] J. Wolpaw and D. McFarland, "Control of a two-dimensional movement signal by a noninvasive brain-computer interface in humans," *Proceedings of the National Academy of Sciences of the United States of America,* vol. 101, p. 17849, 2004.

[6] A. Kübler, B. Kotchoubey, T. Hinterberger, N. Ghanayim, J. Perelmouter, M. Schauer, C. Fritsch, E. Taub, and N. Birbaumer, "The thought translation device: a neurophysiological approach to communication in total motor paralysis," *Experimental Brain Research,* vol. 124, pp. 223-232, 1999.

[7] E. Sellers, D. Krusienski, D. McFarland, T. Vaughan, and J. Wolpaw, "A P300 event-related potential brain-computer interface (BCI): The effects of matrix size and inter stimulus interval on performance," *Biological psychology,* vol. 73, pp. 242-252, 2006.

[8] D. Krusienski, E. Sellers, D. McFarland, T. Vaughan, and J. Wolpaw, "Toward enhanced P300 speller performance," *Journal of Neuroscience Methods,* vol. 167, pp. 15-21, 2008.

[9] J. Park, K.-E. Kim, and S. Jo, "A POMDP approach to P300-based brain computer interfaces", In *Proc Int Conf Intelligent User Interfaces*, Hong Kong, China, Feb 2010.

[10] A. Lenhardt, M. Kaper, and HJ. J. Ritter, "An adaptive P300-based online brain-computer interface", *IEEE Transactions on Neural Systems and Rehabilitation Engineering*, vol. 16, no. 2, pp. 121-130, 2008.

[11] H. Serby, E. Yom-Tov, and G. F. Inbar, "An improved P300-based brain-computer interface", *IEEE Transactions on Neural Systems and Rehabilitation Engineering*, vol. 13, no. 1, pp. 89-98, 2005.

[12] M. Thulasidas, C. Guan, and J. Wu, "Robust classification of EEG signal for brain-computer interface", *IEEE Transactions on Neural Systems and Rehabilitation Engineering*, vol. 14, no. 1, pp. 24-29, 2006.

[13] C. Bell, P. Shenoy, R. Chalodhorn, and R. Rao, "Control of a humanoid robot by a noninvasive brain-computer interface in humans," *Journal of Neural Engineering,* vol. 5, pp. 214-220, 2008.

[14] C. Escolano, J. Antelis, and J. Minguez, "Human Brain-Teleoperated Robot between Remote Places," 2009.

[15] B. Rebsamen, et al., "A brain controlled wheelchair based on P300 and path guidance", In *Proc IEEE/RAS-EMBS Int Conf Biomed Rob Biomech*, pp. 1001-1006, 2006.

[16] I. Iturrate, J. Antelis, A. Kübler, and J. Minguez, "Non-invasive brain-actuated wheelchair based on a P300 neurophysiological protocol and automated navigation", *IEEE Transactions on Robotics*, vol. 25, no. 4, pp. 762-766, Aug 2005.

[17] G. Pfurtscheller, C. Brunner, A. Schlogl, and F. H. Lopes da Silva, "Mu rhythm (de) synchronization and EEG single-trial classification of different motor imagery tasks," *Neuroimage,* vol. 31, pp. 153-159, 2006.

[18] S. G. Mason, G. E. Birch, N. S. Found, and B. C. Burnaby, "A brain-controlled switch for asynchronous control applications," *IEEE Transactions on Biomedical Engineering,* vol. 47, pp. 1297-1307, 2000.

[19] G. Townsend, B. Graimann, and G. Pfurtscheller, "Continuous EEG classification during motor imagery-simulation of an asynchronous BCI," *IEEE Transactions on Neural Systems and Rehabilitation Engineering,* vol. 12, pp. 258-265, 2004.

[20] D. McFarland, L. Miner, T. Vaughan, and J. Wolpaw, "Mu and beta rhythm topographies during motor imagery and actual movements," *Brain Topography,* vol. 12, pp. 177-186, 2000.

[21] J. Millan, F. Renkens, J. Mourino, and W. Gerstner, "Noninvasive brain-actuated control of a mobile robot by human EEG," *IEEE Transactions on Biomedical Engineering,* vol. 51, pp. 1026-1033, 2004.

[22] G. Pfurtscheller and C. Neuper, "Motor imagery activates primary sensorimotor area in humans," *Neuroscience letters,* vol. 239, pp. 65-68, 1997.

[23] X. Pei and C. Zheng, "Classification of left and right hand motor imagery tasks based on EEG frequency component selection."

[24] W.-Y. Hsu, C.-C.Lin, M.-S. Ju, and Y.-N.Sun, "Wavelet-based fractal features with active segment selection application to single-trail EEG data", *J Neuroscience Methods*, vol. 163, pp.145-160, 2007.

[25] T.H. Dat, and C. Guan, "feature selection based on fisher ratio and mutual information analyses for robust brain computer interface", *ICASSP*, 2007.

[26] P. Herman, G. Prasad, T. M. McGinnity, and D. Coyle, "Comparative analysis of spectral approaches to feature extraction for EEG-based motor imagery classification", *IEEE Transactions on Neural Systems and Rehabilitation Engineering*, vol. 16, no. 4, pp.317-326, 2008.

[27] C. Brunner et al., "Spatial filtering and selection of optimized components in four class motor imagery EEG data using independent component analysis", *Pattern recognition letters*, vol. 28, no. 8, pp. 957-964, 2007.

[28] D. J. McFarland, L. M. McCane, S. V. David, and J. R. Wolpaw, "Spatial filter selection for EEG-based communication," *Electroencephalography and clinical Neurophysiology,* vol. 103, pp. 386-394, 1997.

[29] S. L. Marple Jr, *Digital spectral analysis with applications*, Prentice-Hall, Englewood Cliffs, NJ, 1987.

[30] G. J. McLachlan, *Discriminant analysis and statistical pattern recognition*, Wiley-IEEE, 2004.